Article

Design and Implementation of a Programmable Multi-Parametric Five Degrees of Freedom Seismic Waves Geo-Mechanics Simulation IoT Platform

Hasan Tariq [1,*], Farid Touati [1], Mohammed Abdulla E. Al-Hitmi [1], Damiano Crescini [2] and Adel Ben Mnaouer [3]

[1] Department of Electrical Engineering, College of Engineering, Qatar University, 2713, Doha, Qatar; hasan.tariq@qu.edu.qa (H.T.); touatif@qu.edu.qa (F.T.); m.a.alhitmi@qu.edu.qa (M.A.E.A.-H.)
[2] Brescia University, 25121 Brescia, Italy; damiano.crescini@unibs.it (D.C.)
[3] Canadian University Dubai, Dubai, UAE; adel@cud.ac.ae (A.B.M.)
* Correspondence: hasan.tariq@qu.edu.qa; Tel.: +974-50419852

Received: date; Accepted: date; Published:

Abstract: Natural calamities observation, study and simulation has always been a prime concern for disaster management agencies. Billions of dollars are spent annually to explore geo-seismic movements especially earthquakes but it has always been a unique accident. The real-time study of seismic waves, ground motions, and earthquakes always needed a programmable mechanical structure capable of physically producing the identical geo-seismic motions with seismology domain definitions. A programmable multi-parametric five degrees of freedom electromechanical seismic wave events simulation platform to study and experiment seismic waves and earthquakes realization in the form of geo-mechanic ground motions is exhibited in this work. The proposed platform was programmed and interfaced through an IoT cloud-based Web application. The geo-mechanics was tested in the range of i) frequencies of extreme seismic waves from 0.1Hz to 178Hz; ii) terrestrial inclinations from -10.000° to 10.000°; iii) velocities of 1km/s to 25km/s iv) variable arrival times 1us to 3000ms; v) magnitudes M1.0 to M10.0 earthquake; vi) epi-central and hypo-central distances of 290+ and 350+ kilometers. Wadati and triangulation methods have been used for entire platform dynamics design and implementation as one of key contributions in this work. This platform is as an enabler for a variety of applications such as training self-balancing and calibrating seismic-resistant designs and structures in addition to studying and testing seismic detection devices as well as motion detection sensors. Nevertheless, it serves as an adequate training colossus for machine learning algorithms and event management expert systems.

Keywords: Motion sensors; seismic sensing; Wadati method; earthquakes; programmable; simulation; test bench; calibration; machine learning; IoT platform.

---

1. Introduction

The natural disasters and accidents happen annually across the globe with earthquake and floods being most devastating and alarming on the loss and damage benchmarks. The casualties reported by natural calamities, i.e. 564.4million were the highest in 2006 as compared to the last 10 years [1], amounting to 1.5 times its annual average 224 million. The global natural disaster economic damages, i.e. US$ 154 billion scrutinized in the last year as the fifth costliest since 2006, i.e. 12% above the 2006-2015 annual average registered in CRED database. Earthquake or seismic events have proven to be the most obvious and recurring in all [2] the natural disasters i.e. 14,568 in 2018. The death toll of 2,256 on September 28, 2018 in Indonesia was at the top of charts.

Domain realization and perception assistance is the foremost constraint in all simulation platforms design and implementations. In geo-seismic domain, a plethora of contributions were observed in simulation area from theoretical and mathematical modelling aspect. The Tullis group

 doi:10.20944/preprints201907.0324.v1

simulator RSQSim [3] was appreciable for fault-friction modelling, fully dynamic single-event simulations, rate- and state dependent friction(RSF) modelling with a gap of wave modelling and ground motions realization. The ALLCAL [4] was one of the earthquake simulators developed by scientists of the Southern California Earthquake Center(SCEC) and belonged to Tullis group of simulators. The ALLCAL used the Triangulation rule for the geometrical modelling and estimation of stresses and displacement to approximate fault friction and elastodynamics at very abstract level had a gap of mechanical implementation and core geo-seismic realization. The Viscoelastic earthquake simulator for San Francisco Bay region [5] was very noticeable approach towards seismicity functions with a gap of real surface motion kinematics, i.e. seismic waves and arrival times. The Virtual Quake(VQ) earthquake simulator [6] was a simulation-based forecast of the El Mayor-Cucapah region and evidence of predictability in simulated earthquake sequences was a successor of Virtual California(VC) can be used for forecasting and training mechanics. The gap of physical design and implementation was very prominent in VQ contribution. The physics-based earthquake simulator replicated seismic hazard statistics across California [7] and compared its results with UCERF3(Uniform California Earthquake Rupture Forecast, version 3) and RSQSim reliant on parameterized ground motion models(GMMs). The current state earthquake simulation [8] contribution also had gaps in geo-seismic realization and its relationship with geo-mechanics implementation. The gaps of geo-seismic realization as mechanical platform for physical implementation were observed in all [3-8] contributions.

An effective early warning and disaster management(EWDM) needs a trustable ground motion simulator for training and realization purposes. The contribution [9] was a generic earthquake test and needed to be improved mechanically and electronically. The world's largest ground motion simulator(GMS) [10] was jointly owned by the Civil Defense College and Ankara Search & Rescue Unit operated at 380V and delivered a maximum frequency of 12Hz and velocity of 80 cm/s needed serious attention from the design of skeleton, power efficiency, and size. The second largest earthquake facility [11] in the world with a payload 1,200 tons, maximum velocity 200 cm/s, and maximum displacement +/- 1 m for horizontal excitation and maximum velocity 70cm/s, maximum displacement +/- 50cm for vertical excitation to realize destructive ground motion was limited to a shake table i.e. P-waves simulation needed improvement in design, mechanic, and electronics for S-waves. The myQuake [12] was energy and payload optimized and had P-wave capabilities but needed improvement in characteristic frequencies and amplitudes benchmarks. The seismic events variable rotation test bench [13] with angular acceleration 2~500 rad/s, angular velocity 0.0002~35 rad/s, angular resolution 10:1700, frequency range 0.001~1000 Hz and payload 5kg needed advancement in frequency, mechanical design, power economics, and IoT. The GG SCHIERLE [14] shake table with spring-loaded mechanism and capable of vibration of 2.99Hz frequency and 3mm amplitude needed rework and improvement in seismic definitions, drive electronics, mechanical structure, IoT and results detailing. The State Key Laboratory for Disaster Reduction in Civil Engineering, Tongji University had a reference shake table used in [15] with carrying capacity of 20kg required seismic definitions, drive intelligence, wave parametric design, IoT and data set import capabilities. The [16] shake table with motor shaft based motion control mechanism in UC, Berkley needed IoT, web interface and data set import support features. The gaps of programmable multi-parametric geo-seismic to geo-mechanics motion controls realization and integration in web interface for remote simulation were observed all [3-16] contributions.

Dedicated and comprehensive efforts were observed in automation centered electro-mechanical design full scale shake table [17] by NHERI Tall Wood Project Team with gaps in parameter settings and upload from remote location and detailed programmable geo-mechanics control. The programmability feature in Fuzzy-PLC based earthquake simulator [18] was a revolutionary add-on but till gaps of geo-seismic realization to motion commands for motors as well as user-interface(UI) as human machine interface(HMI) was the limitation. The multi-purpose earthquake simulator [19] and a flexible development platform for actuator controller design had only P-wave simulation capability was very basic design. The flexible IoT platforms [20-23] based design and implementation efforts had very appreciable high-resolution bi-axial displacement, acceleration, and vibration

Preprints (www.preprints.org) | NOT PEER-REVIEWED | Posted: 29 July 2019 doi:10.20944/preprints201907.0324.v1

sensing capabilities and needed improvement in multi-parametric gap of mechanical actuation as well as geo-seismic realization. The 4-DoF multi-parametric design [24] needed thorough improvements in geo-seismic domain realization as well as IoT features [25] like web to actuator control accomplished in this work.

The nine target gaps that needed to be addressed were mechanical design in terms of, i) more degrees of freedom(DOF); ii) multi-parametric geo-seismic realization; iii) geo-mechanics simulation capabilities by motion control intelligence; iv) power efficiency; v) data sets upload and download options; vii) web and IoT controls; viii) accuracy in P, S, Raleigh(R), and Love(L) waves; as well as ix) customizable ground motions generation.

This work focuses on a complete programmable multi-parametric 5-DOF seismic wave ground motions simulation platform (GMSP) for P, S, Rayleigh, and Love waves with the novel:

- Multi-parametric Geo-Seismic Realization Engine(GRE) Design and Implementation
- Programmable 5-DOF Seismic Machine Apparatus(SMA) Design and Fabrication
- Motion Control System (MCS) or Mechatronics System Assembly and Programming
- IoT Web Interface Design and Implementation with Seismic Parameters and Data Integration

2. GMSP Design and Implementation

A GMSP is a multi-sensing, multi-parametric, and programmable actuators platform that gives the exact realization of real seismic events by mathematical formulations. The first step is designing any physical world simulation system is to realize the domain parameters. The second step is the nearest possible physical model that resembles the real world application. In this third step, sensors are selected that realize the domain variables. The fourth step is the flexibility or programmability of actuators to create respective events. The entire conceptual model of this work in figure 1.

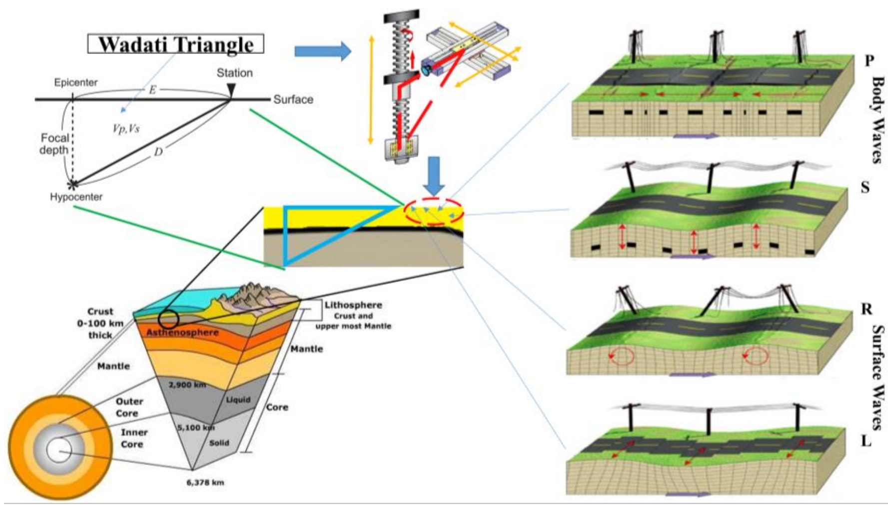

Figure 1. Overall Conceptual Layout of GMSP

2.1. Multi-parametric Geo-Seismic Realization Engine Design and Implementation

The objective of GRE was to convert seismological variables and parameters into actuator commands and sense them to ensure the accuracy of the simulation system. In seismology, there are two basic types of waves i.e. body waves and surface waves with sub-types of each. Body waves have two sub-types i.e. primary (P), secondary(S) and surface waves have Rayleigh(R) and Love(L) waves. For a sensing system, seismic waves are very specific ground motion events that need to be sensed in x, y, and z directions as D_X, D_Y, and D_Z. In figure 1, it can be observed that seismic waves study is focused on ground motion and anomalies in lithosphere and crust only. The point where the seismic fault occurs and generates the earthquake is called hypocenter(C_H) and its perpendicular point on earth surface is called epicenter(C_E). The point where seismic variables are observed is called a seismic station(S_S). The hypocenter and epicenter measurement assists in the computation of magnitude(M) and energy(E) of earthquakes. After seismic motion generation, the triangulation method is used to find the epicenter as the first step. Three seismic stations are a mandatory requirement for the triangulation method. The P, S, R and L waves can be sensed any high-sampling and precision bi-axial motion sensors. The waves velocity or motion needs accelerometers and angular displacement needs inclinometers tactically oriented in x, y and z-axis. The conversion of seismic variables into motion control commands in given below in Table I. Let the five motors be first horizontal shaft motor be M_{HS1}, second horizontal shaft motor be M_{HS2}, first vertical shaft motor be M_{VS1}, second vertical shaft motor be M_{VS2}, and third vertical shaft motor be M_{HV3}.

Table 1. Realization Geo-Seismic Events as Motion Control Commands

Geo-Seismic Domain		GMSP Motion Control Domain
Event Patterns	P-Waves Pattern(P_{EVENT})	M_{HS1} (CW + A-CW)
	S-Waves Pattern(S_{EVENT})	M_{VS1} (CW + A-CW)
	R-Waves Pattern(R_{EVENT})	M_{VS1} (CW) + M_{HS1} (CW) and M_{VS1} (A-CW) + M_{HS1} (A-CW)
	L-Waves Pattern(L_{EVENT})	M_{HS1} (CW) + M_{HS2} (CW) + M_{HS1} (A-CW) + M_{HS2} (A-CW)
	Earthquake Pattern(E_{EVENT})	$T_{PRE} + P_{EVENT} + T_{POST-P} + S_{EVENT} + T_{POST-S} + R_{EVENT}$ Or $T_{PRE} + P_{EVENT} + T_{POST-P} + S_{EVENT} + T_{POST-S} + L_{EVENT}$
Quantity of Patterns	Number of Waves(N_{WAVES})	n * $W_{EVENT}(P_{EVENT}, S_{EVENT}, R_{EVENT}, L_{EVENT})$
	Number of Earthquakes(E_{EQKS})	n * E_{EQKS}
Timers of Patterns	Arrival Time of P-Wave(T_{AP})	T_{PRE}
	Arrival Time of S-Wave(T_{AS})	$T_{AP} + T_{WP-P} + T_{POST-P}$
	Arrival Time of Rayleigh Wave(T_{AR})	$T_{AS} + T_{WP-S} + T_{POST-S}$
	Arrival Time of Love Wave(T_{AL})	$T_{AS} + T_{WP-S} + T_{POST-S}$
	Delay(T_{POST})	Post-Delay in Motors Commands
	Duration of Waves Pattern(T_{WP})	$N_{WAVES} * T_W$
	Duration of Earthquake(T_{EQK})	$T_{PRE} + T_{WP-P} + T_{POST-P} + T_{WP-S} + T_{POST-S} + T_{WP-R}$ Or $T_{PRE} + T_{WP-P} + T_{POST-P} + T_{WP-S} + T_{POST-S} + T_{WP-L}$
Magnitude of Pattern	Peak to Peak Amplitude of Waves(A_W)	$2 * \sum_{i=0}^{n} P_{LS}$
	Magnitude of Earthquake (M_{R-EQKS})	log(A_W/T_{EQK}) or
Duration of a Single Wave	Time period of Waves(T_W)	Steps Timer for movement (CW + A-CW)
Frequency of a Single Wave Pattern	Frequency of a Wave(F_W)	1 / T_W
Distance Travelled	Distance Traveled by Waves(D_W)	Total Steps * T_W
	Distance Traveled by Unit Earthquake(D_{EQKS})	$D_{W-P} + D_{W-S} + D_{W-R}$ or $D_{W-P} + D_{W-S} + D_{W-L}$
Velocity of Waves	Velocity of P-Waves(V_P)	D_{W-P} / T_{W-P}

Preprints (www.preprints.org) | NOT PEER-REVIEWED | Posted: 29 July 2019 doi:10.20944/preprints201907.0324.v1

(can be X and Y)	Velocity of S-Waves(V_S) Velocity of R-Waves(V_R) Velocity of L-Waves(V_L)	D_{W-S} / T_{W-S} D_{W-R} / T_{W-R} D_{W-L} / T_{W-L}
Impact of P-Waves w.r.t to Equator and Poles	Angle of Incidence P-Waves(Θ_P) (can be X and Y)	Average Angle of P-Cluster where angle and acceleration is similar
Impact of S-Waves w.r.t to Equator and Poles	Angle of Incidence P-Waves(Θ_S) (can be X and Y)	Average Angle of S-Cluster where angle and acceleration is similar
Hypocenteral Distance	Hypotenuse of Wadati Triangle (H_{WT})	B_{WT} / {cos((Θ_S+ Θ_P)/2)}
Epicentral Distance	Base of Wadati Triangle (B_{WT})	(T_{AS} - T_{AP}) * {(V_P* V_S)/ (V_P - V_S)}
Epi-Hypo Distance	Perpendicular of Wadati Triangle (P_{WT})	B_{WT} / {sin((Θ_S+ Θ_P)/2)}
Location of S_S	GPS Coordinates (Y°N, X°E)	Longitude and Latitude Values
Location of (C_H, C_E)	GPS Coordinates of Offset = (B_{WT}) from S_S ((Y°N, X°E)	S_S (Y°N, X°E) + (B_{WT} [sin{(Θ_S+ Θ_P)/2}]°N, B_{WT} [cos{(Θ_S+ Θ_P)/2}]°E)

In table 1, all the information regarding GRE is given. Clockwise and anti-clockwise rotation is expressed as CW and A-CW. Further details can be read from references cited in the introduction.

2.2. Programmable 5-DOF Seismic Machine Apparatus Design and Fabrication

The mechanics of seismic events and earth typography prevails the design of SMA measurements and design constraints. The extreme values for seismic variables in top 3 earthquakes i.e. the Chile Earthquake (1960) with M9.5, the Atlanta earthquake (1964) with M9.2 and the Indian Ocean earthquake (2004) with M9.1 have been employed as standard design parameter set. The SMA design process has been divided into two sections:

- SMA Static Parts Sizing and Dimensions
- SMA Dynamic Parts Sizing and Dimensions

2.2.1. SMA Static Parts Sizing and Dimensions

The epicenter, hypocenter, focal depth, triangulation area, and seismic station are the static locations on the map thus their mechanical equivalents will also be static components. The global datasets on IRIS and USGS were used to specify the limits and extent of parts designed and used for mechanical structure. Considering into account the top 3 earthquakes i.e. 1960 Chilean earthquake in Valdivia with Richter M9.5, 1964 Alaska earthquake with Richter M9.2~9.3 and 2004 Indian Ocean earthquake in Sumatra with Richter M9.1, the static parts sizing was accomplished. The re-scaled sizing was performed in the same ratios to streamline the dimensions of static parts in GMSP given in table 2.

Table 2. GRE Dimensions for SMA Static Parts

Metadata	**Top 3 Mega Earthquakes**			**SMA Parts Sizing**	
Name	**Valdivia, 1960**	**Alaska, 1964**	**Sumatra, 2004**	**Structure**	**Dimensions (Approx)**
Epicentral Distance	150 km (Calc)	141 km (Calc)	157 km (Calc)	**Assembly (AE)**	35 ~ 146 mm
Hypocentral Distance	153 km (Calc)	143 km (Calc)	160 km	**Assembly (AD)**	50 ~ 150 mm
Focal Depth	33 km	25 km	30 km	**Assembly (AFD)**	29.33 ~ 34.33 mm

Magnitude	9.5	9.2	9.1	**Oscillation Tolerance**	Hinged Joint (MS + Acrylic)
Triangulation Area	10 km E 90 km W 120 km N	20 km N 125 km E 64 km W	Not Found	**GMSP Bed (GB)**	300mm Side A 300mm Side B 300mm Side C

The 3D models of SMA static parts were designed in AutoCAD and are shown in figure 2. The word "(Calc)" means it was mathematically calculated using Pythagoras theorem and "Not Found" means that we could not found any reliable source of information for this field. The dimensions are approximated from the average of parameters of top 3 earthquakes.

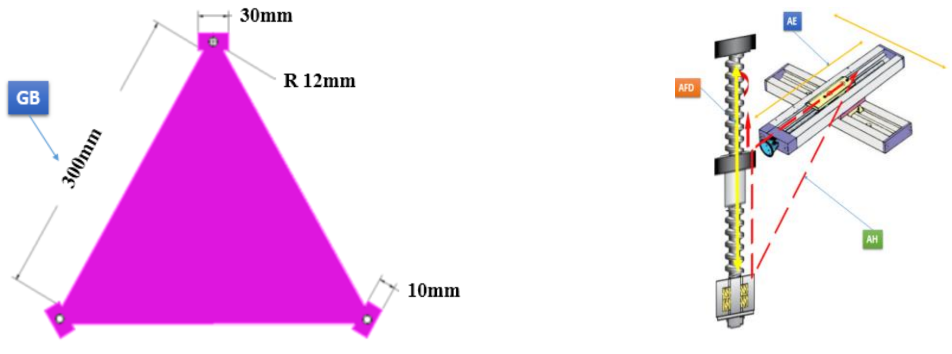

(**a**) (**b**)

Figure 2. Core components of SMA Static Parts 3D Model as (**a**) GMSP Bed Dimensions; and (**b**) Assemblies (AE, AD, AFD)

In figure 2, it can be seen that initially static parts have been designed on the basis of realistic approximation of geology of top 3 earthquakes with scaling ratio of 0.33mm = 1km means GMSP bed is capable of simulating 1000km crust surface. The three corners represent 3 seismic stations in accordance with the Wadati triangle method and triangulation rule for geo-seismic estimations.

2.2.2. SMA Dynamic Parts Sizing and Dimensions

The dynamic parts include gears, shafts; and motors. The seismic waves velocities, frequencies, and wavelengths have led dynamic parts estimation. Considering into account of the standard seismology literature referred in the introduction section, the dimensions of the dynamic parts are given in table 3. The seismic velocities were governed by lead screws coupled with bi-polar stepper motors, frequencies by rotation per second(RPM) of motors by full-stepping and micro-stepping and wavelengths by the pitch of lead-screws and number of threads traveled per second. The unit pitch was the minimum unit of velocity for any wave and half times of rated RPM stepper was expected frequency generated by stepper motor as a multi-parametric actuator.

Table 3. GRE Dimensions for SMA Dynamic Parts

Metadata	Seismic Waves				SMA Parts Sizing	
Parameters	**P**	**S**	**R**	**L**	**Structure**	**Dimensions**
Velocity	5~8 km/s	3~4 km/s	2~4.2 km/s	2~4.4 km/s	**Lead (TPS)**	2~8
Frequency	4~8 Hz	1.5~3 Hz	0.03~0.7 Hz	0.05~0.5 Hz	**Motor(RPM/2)**	16~32
Wavelength	5m~50 km	30m~500km	30 to 1000 km		**Length(Screws)**	0.05~500mm

The frequencies have been achieved using revolution per minute, wavelength through the amplitude of vibration by scaling radius of earth R = 6.371km i.e. circumference, C = 40,075 km. The average of wavelength of P-wave, λP = 25km and S-wave, λS = 235km, diving it into least count of a measurement instrument C/ λ = (1603, 170.5) means that for GMSP the minimum displacement for P-wave is dP = 1.603cm and S-wave is, dS = 0.17cm to realize the comparative ground motions. For this,

Preprints (www.preprints.org) | NOT PEER-REVIEWED | Posted: 29 July 2019 doi:10.20944/preprints201907.0324.v1

two different lead screw assemblies were selected with stepper motors with step angles 1.8° and 5000RPM, 20 steps per revolution for P-wave to achieve dP and 200 steps per revolution for dS. The desired assembly was designed in AutoCAD as 2D and 3D and given in fig 2 as a 4 DOF motion platform. The considerations like epicenter and seismic center have been kept in account while designing the mechanical assembly for GMSP.

Table 4. Stepper Motor and Lead Screw Specifications

Parts	Stepper Motors Specs			Lead Screws Dimensions				
Motors	**RPM**	**Steps**	**Step-Angle**	**Screws**	**Pitch**	**TPI**	**Length**	**Diameter**
Type 1	>32	200	1.8°	**Type 1**	1.25mm	20	500mm	8mm
Type 2	>16	18	20°	**Type 2**	3mm	8.5	140mm	3mm

Table 4 is complete interpretation and derivation from table 3, i.e. geo-seismic mechanics to the electromechanical domain. The motors and lead screws parameters are computed by maximum possible limits of high flexibility in the precision of the system.

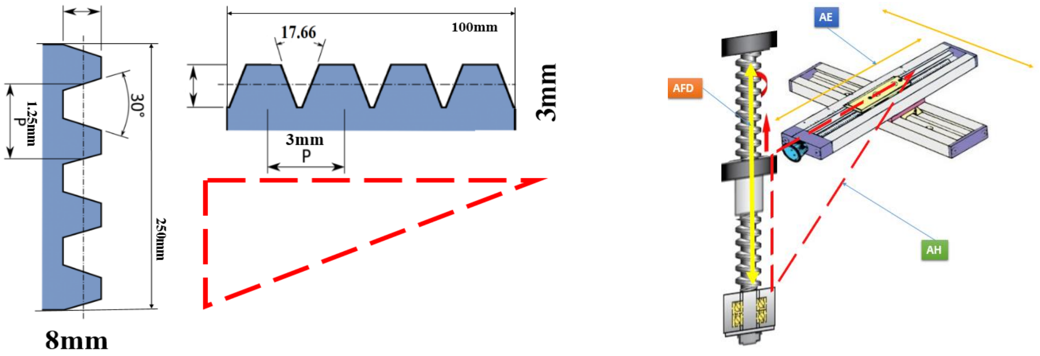

(**a**) (**b**)

Figure 3. Description of SMA Dynamic Parts Mechanical CAD and 3D Model as (**a**) Lead Screws Design; and (**b**)Specifications Assemblies (AE, AD, AFD)

In figure 3, it can be seen that initially dynamic parts have been designed on the basis of realistic approximation mechanics of seismic waves from IRIS and USGS database. The pitch 1.25mm assists in 4km surface movement and 3mm in 9km as per scaling defined in table 3 i.e. single revolution of type 1 motor created motion of 4km and type 2 motor created 9km i.e. at max RPM will produce velocities of 1200km/min and 27000km/m. This speed is much more than realistic seismic velocities. The overall assembly is given in figure 4.

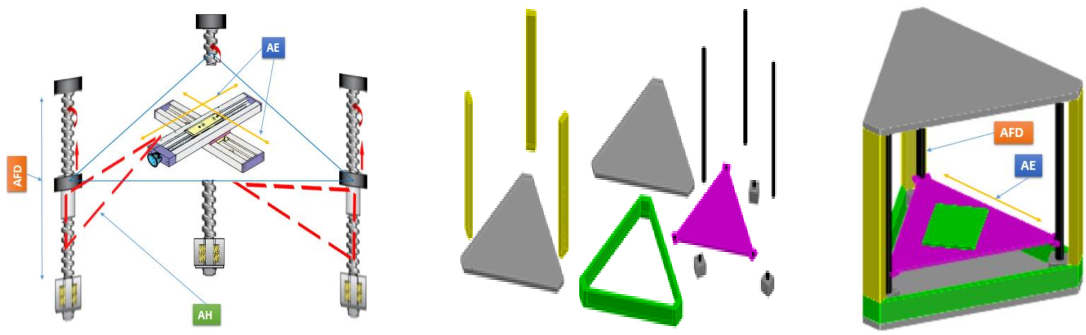

(**a**) (**b**) (**c**)

Figure 4. Exhibition of Overall GMSP Assembly and 3D Model as (**a**) Internal Assembly; (**b**) Overall Parts 3D Model (**c**) Assembled GMSP

In figure 4, the internal assembly is scaled and oriented according to the triangulation and Wadati method based on real-world calculations. The external assembly serves the purpose of

Preprints (www.preprints.org) | NOT PEER-REVIEWED | Posted: 29 July 2019 doi:10.20944/preprints201907.0324.v1

alignment and minimizing kinematic disturbances due to linear and angular motions and resulting vibrations. The entire concept of GSMP is given in the figure below.

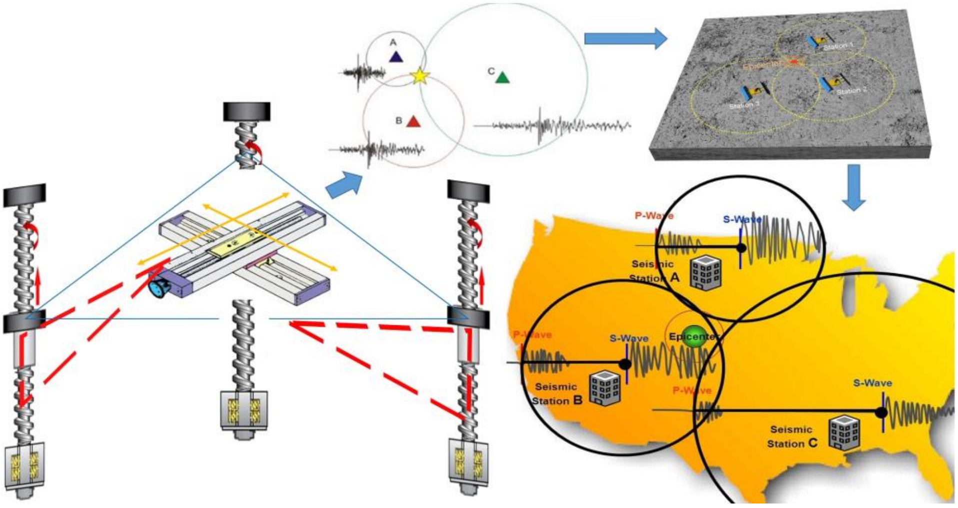

Figure 5. The Comprehensive Realization of GMSP

In figure 5, the overall system is defined with geo-seismic reference and its operation capacity as a three station simulation platform as three equidistant assemblies (AE, AD, AFD) for A, B and C geo-locations.

3. Motion Control System (MCS) or Mechatronics System Assembly and Programming

The GMSP MCS consists of three subsystems the geo-seismic heterogeneous sensing node, geo-seismic actuator-drive system and MCS controller with IoT enablement capabilities. The GMSO at boot up is initialized with a perfectly static structure. The first step after booting is normalizing the SMA to 0 tilt-angle and move the GB to origin so that there are no offsets by the help of instrumentation support. In the second step, the GMSP gives an indication of "Ready" and is ready to take user inputs. The three components of MCS are:

- Geo-seismic heterogeneous-sensing node(GHN)
- Geo-seismic mechanics actuators-drive system (GMAS)
- GMSP MCS Controller

3.1. Geo-seismic heterogeneous-sensing node(GHN):

The block diagram of GHN is given in figure 6 focusing on the measurement requirements in table 3. A bi-axial accelerometer ADXL203 has been used for heterogeneous sensing i.e. acceleration and as well as tilt-angle measurements.

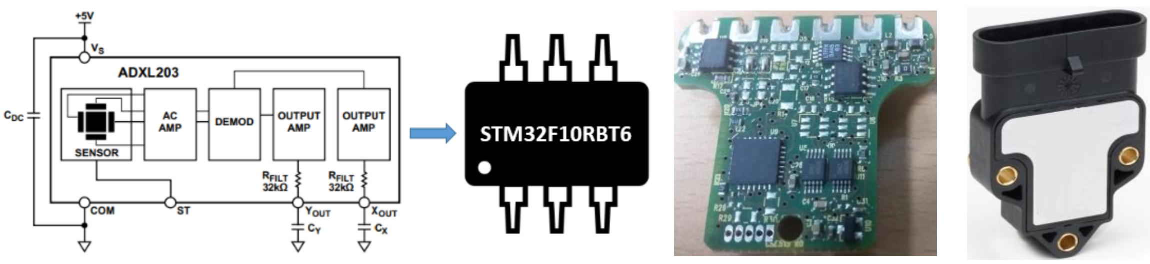

(**a**) (**b**)

Figure 6. The GHN Version 0 as (**a**) GHN Architecture ; and (**b**) GHN Fabrication.

 doi:10.20944/preprints201907.0324.v1

In figure 6, the STM32F10RBT6 (32-Bit microcontroller with CAN-Open Transceiver and 12-Bit ADC with a sampling rate of 1us) is interfaced with ADXL203 using to two ADC channels to constitute one GHN as per (a) and PCB as wells as IP68 enclosure is displayed in (b).

3.2. Geo-seismic mechanics actuators-drive system (GMAS)

The bipolar stepper motors type1 and type2 specified in table 3 are shown in figure 7 with respective motor drives i.e. A4988 with micro-stepping capabilities. The RPM and acceleration programming was also a novel task performed in this work for geo-mechanics. The motion control system consists of an ESP32 an Xtensa II 32-Bit SoC coupled with A4988 stepper drivers with micro-stepping capabilities and 12V/2A power supply drive for bi-polar stepper motors. The overall system layout is given in fig 3.

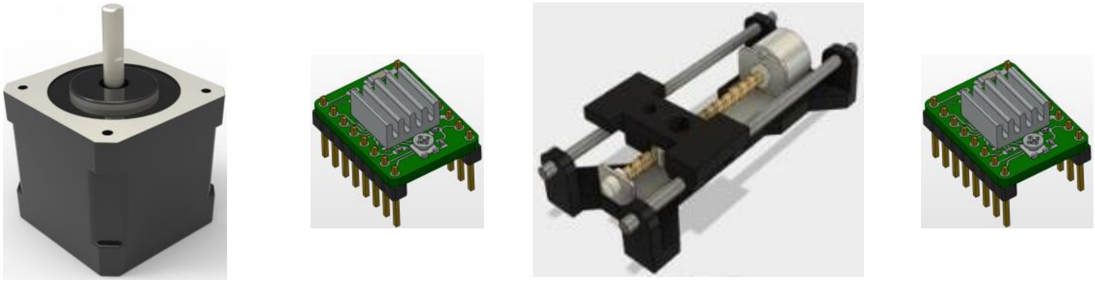

i. Bi-polar Stepper Motor (12V/0.5A) ii. A4988 Motor Driver iii. Bi-polar Stepper motor (12V/0.12A) iv. A4988 Motor Driver

(**a**) (**b**)

Figure 7. The GMSP Motors and Drives as (**a**) Type 1 Motor Drive System; and (**b**) Type 2 Motor Drive System.

Three bi-polar type1 for vertical movements and 2 bi-polar type2 for horizontal motions were used in GMSP.

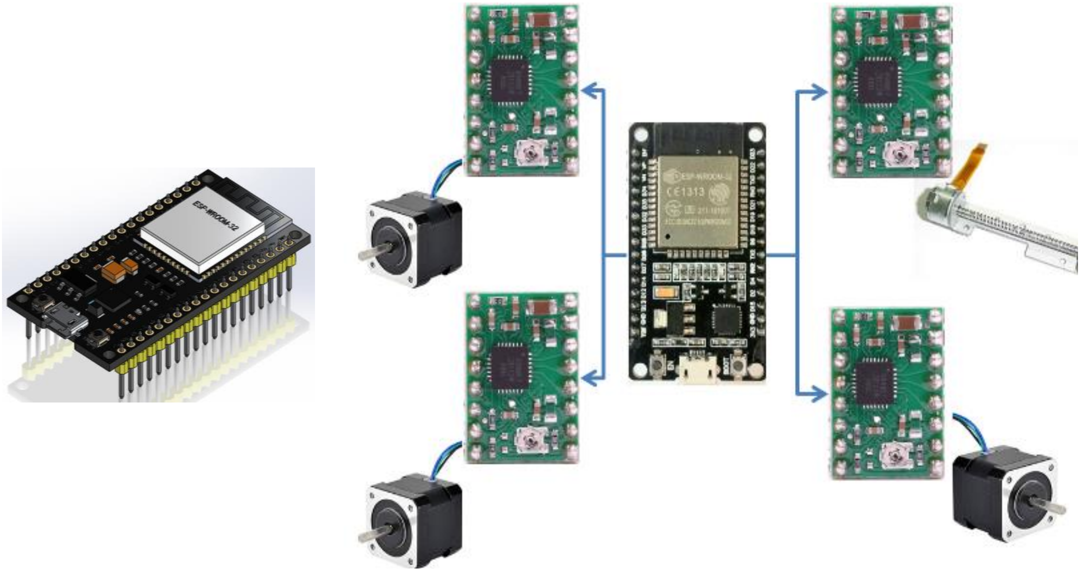

(**a**) (**b**)

Figure 8. The GMSP Motion Actuation System as (**a**) Xtensa II 32-Bit SoC (ESP32); and (**b**) Motion Control System Layout.

In figure 8, it is prominent that a five joint system is powered using 5 stepper motors driven by five A4988 stepper drivers controlled through a single ESP32.

Preprints (www.preprints.org) | NOT PEER-REVIEWED | Posted: 29 July 2019 doi:10.20944/preprints201907.0324.v1

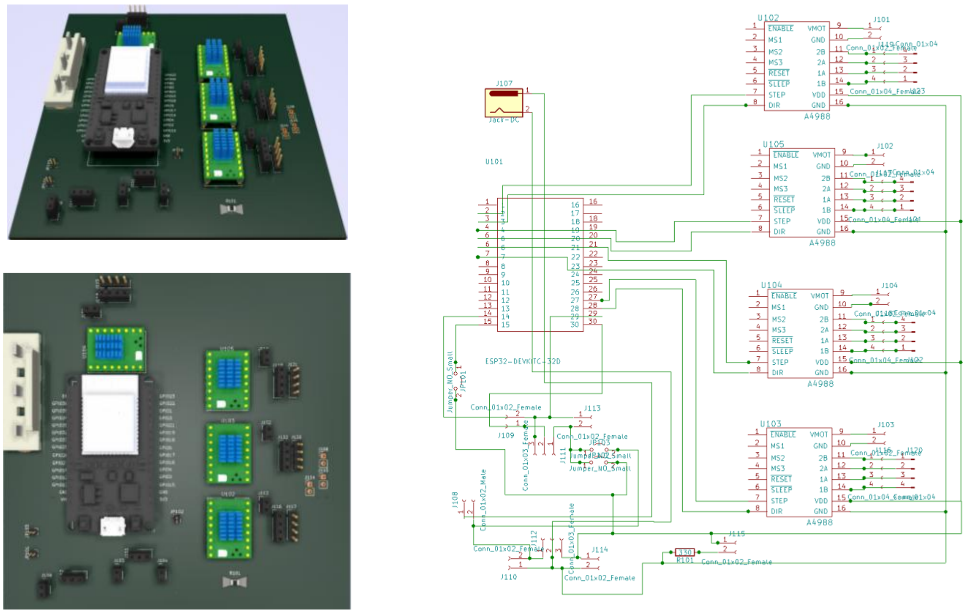

(**a**) (**b**)

Figure 9. Layouts of the GMSP Motion Actuation System designed in KiCAD and FreeCAD as (**a**) PCB Layout Top Views (MCS); and (**b**) Motion Control System Schematics.

A complete GMAS MCS motherboard is shown that enables the entire GMSP is displayed in figure 9. The 3D view of the PCB of the GMSP MCS motherboard is displayed in figure 9(a) and detailed schematics in figure 9(b) sum up the contribution. Two further novelties in this work are schematic symbols, PCB footprints designs, and integration of their 3D models designed in FreeCAD with KiCAD footprint designer module.

3.3. GMSP MCS Controller

The GMSP MCS controller has three core components that are being used for overall GMSP:

- SMA Orientation Neutralizer(SON).
- SPIFFS (Serial Peripheral Flash File System) for a web interface for 3 pages.
- GRE SSG (Seismic Sequence Generator) for OTA firmware.

The control algorithm of the GMSP MCS is given in figure 10. The GMSP MCS follows a sequential methodology of operations given as:

1. When System is powered on it takes inputs from GHN and brings itself into zero “g” condition i.e. removes all the initial value offsets using SON mechanism. Motors operate till it's zero acceleration and displacement at 0° tilt.

2. After SON operations, the access point is created, then AP is created after the acquisition of IP address. After a stable web server creation, the GMSP loads associated pages from SPIFFS for its user interactive web interface explained in later sections.

3. The GRE is stored as a binary code in firmware of SoC and is ready to receive user commands that simulate geo-mechanics by SMA actuated by MCS.

Preprints (www.preprints.org) | NOT PEER-REVIEWED | Posted: 29 July 2019 doi:10.20944/preprints201907.0324.v1

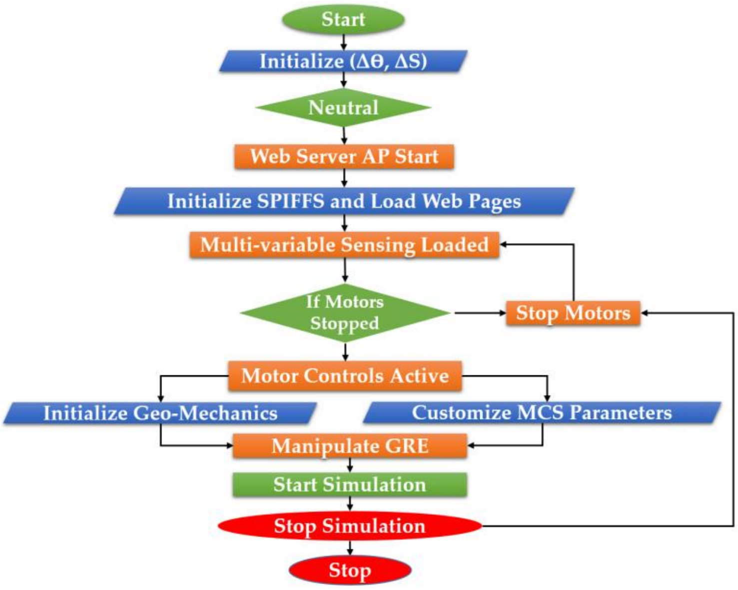

Figure 10. Flowchart of GMSP MCS Control Algorithm

Figure 10, the control algorithm of MCS and very self-explanatory from start till end. Safety operation in MCS is very vital that is neutralizing and stopping the motors by feedback control from GHN.

4. IoT Web Interface Design and Implementation with Seismic Parameters and Data Integration

The IoT web interface gives full flexibility in real-time geo-seismic sensing at the 100Hz sampling frequency, seismic waves and earthquake simulation by GMSP actuation, customized geo-seismic ground motion stimulus generation. HTML, CSS, and JavaScript were used to create user-friendly interfaces comprised of 4 web pages stored in SPIFFS of SoC. The four unique pages have 4 unique functions explained below:

- Page 1: GHN Dashboard
- Page 2: Geo-Seismic Mechanics Actuators-Drive System (GMAS) Workbench
- Page 3: GMSP Motion Control System(MCS) Stimulus Dataset Generator

When the system boots it creates an access point where all the users can connect to access the controls given on web named “NPRP8 Seismic Simulation Rig”.

The HTML and CSS component that is being used as a frontend for user interaction is stored in SPIFFS and the main code with Web Server, AP, motor control instructions and wave generation functions in C are stored as SSG. The Page 1 i.e. GHN dashboard it active all the time and is displaying values as 100Hz refresh rate to inform the current state of X, Y tilt and acceleration. Page 2 has two portions one is dedicated for stored seismic waves simulation and the second part is earthquake simulation based on detailed data-set format required by GMSP that can be converted into motor controls. The USGS and IRIS datasets have to first convert into GMSP format. The datasets found on the cloud were having gaps and missing values. The extensive workout was required for the flawless formulation of IRIS and USGS datasets to be made adaptive with GMSP operational parameters. Page 3 is geo-seismic domain based control form with all the parameter setting and simulation flexibility.

Preprints (www.preprints.org) | NOT PEER-REVIEWED | Posted: 29 July 2019 doi:10.20944/preprints201907.0324.v1

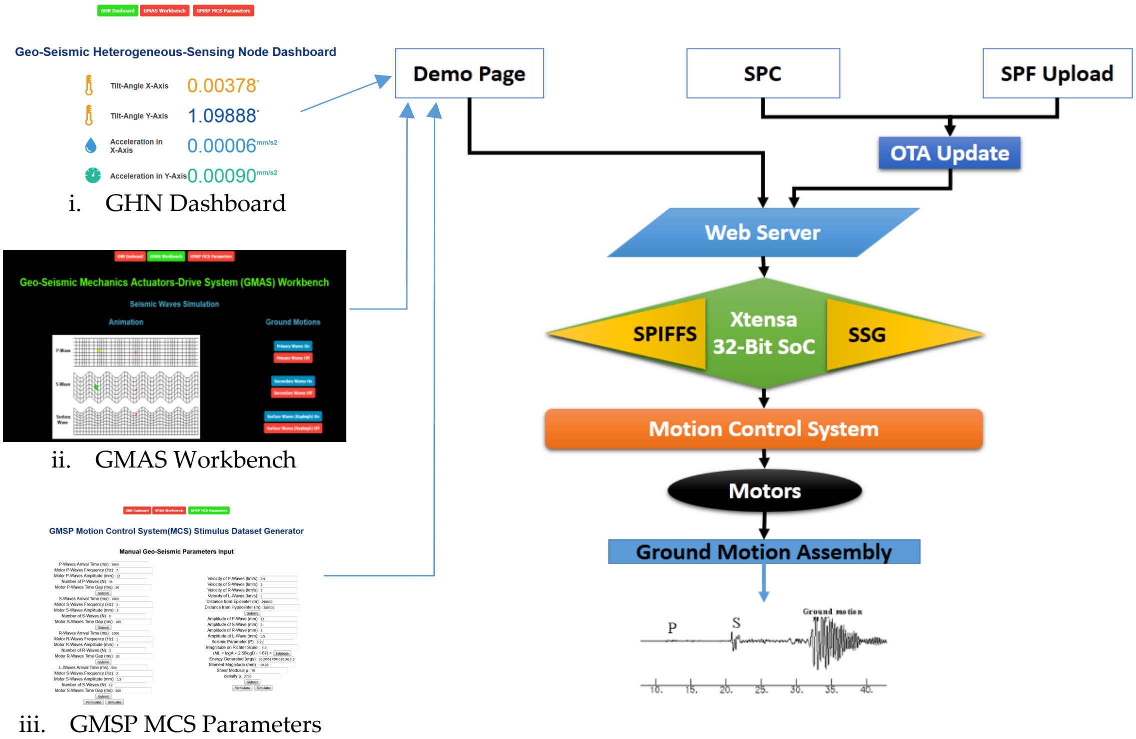

(a) (b)

Figure 11. Description of GMSP IoT Web Platform as (**a**) Demo Pages; and (**b**) IoT Web Flow Diagram.

The first step after booting is normalizing the SMA to 0° tilt-angle and move the GB to origin so that there are no offsets by the help of instrumentation support. In the second step, the GMSP gives an indication of "Ready" and is ready to take user inputs. The three pages of GMSP Web-based hardware management system are:

5. Results and discussion

The GSMP was assembled for performing the experiments as shown in fig 6. The experiment has been set up with a bi-axis accelerometer node with 14-bit resolution also designed and fabricated in our previous works [13-15].

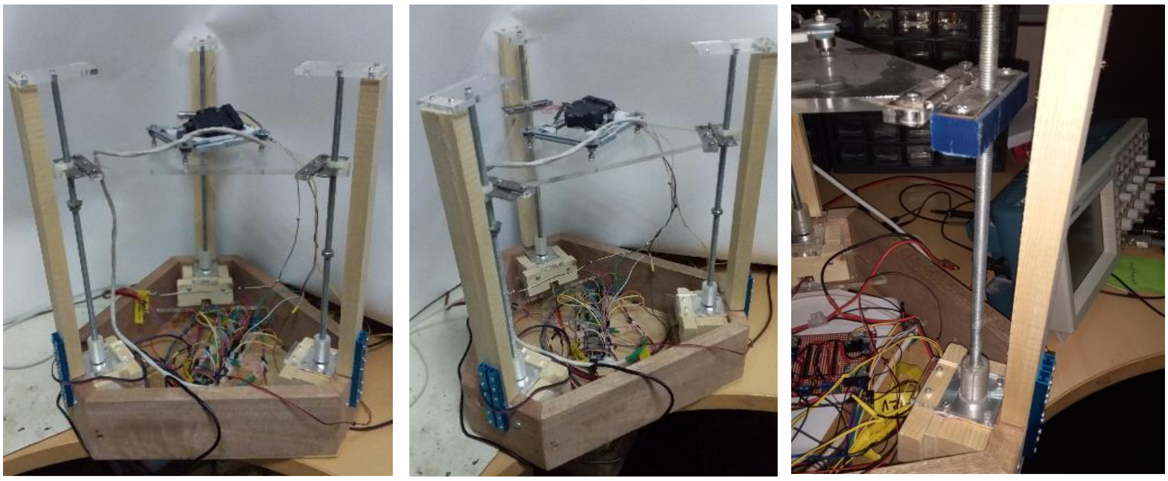

(a) (b)

Figure 12. Photographs of Physically Assembled SMA of GMSP as (**a**) Two views of Physically Assembled GMSP Photographs; and (**b**) Single (B_{WT} and P_{WT}) Station Manipulator.

Preprints (www.preprints.org) | NOT PEER-REVIEWED | Posted: 29 July 2019 doi:10.20944/preprints201907.0324.v1

The results were observed from three sources, i.e. the GHN dashboard, Tektronix TDS 2014 oscilloscope and MATLAB serial input. The GMSP results are very fertile and perceivable by seismologists and geologists.

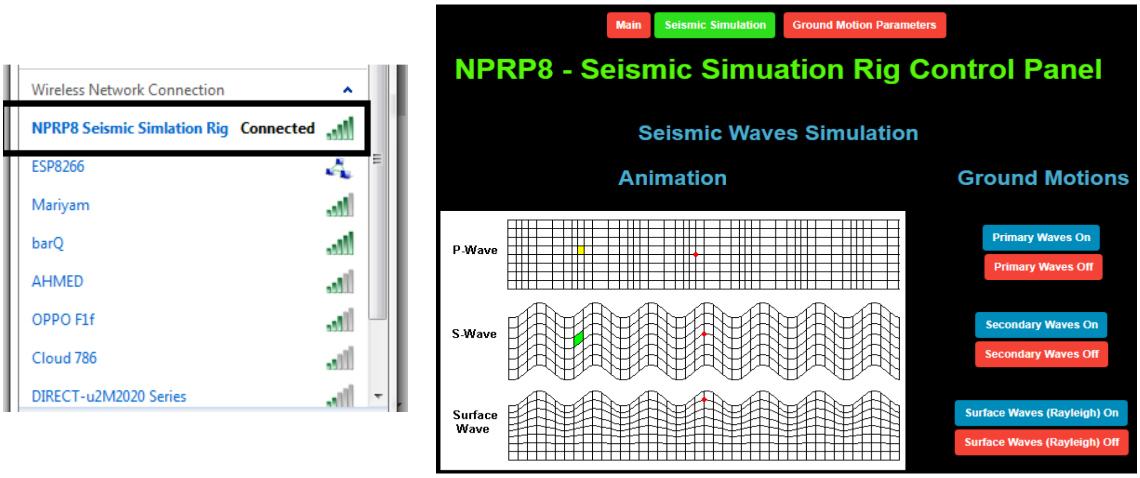

(**a**) (**b**)

Figure 13. IoT Web Interface of GMSP as (**a**) AP Mode for Web Server Access; and (**b**) Home Page of GMSP IoT Platform.

The first indication for user interaction is the visibility of AP in wireless networks as shown in figure 13. After connecting to the AP the user needs to give IP of the gateway from network settings in the URL text field of web browser i.e. 192.168.1.1:81. This opens the GHN dashboard with current values. All the GHN values must be 0 to start the operation of GMSP.

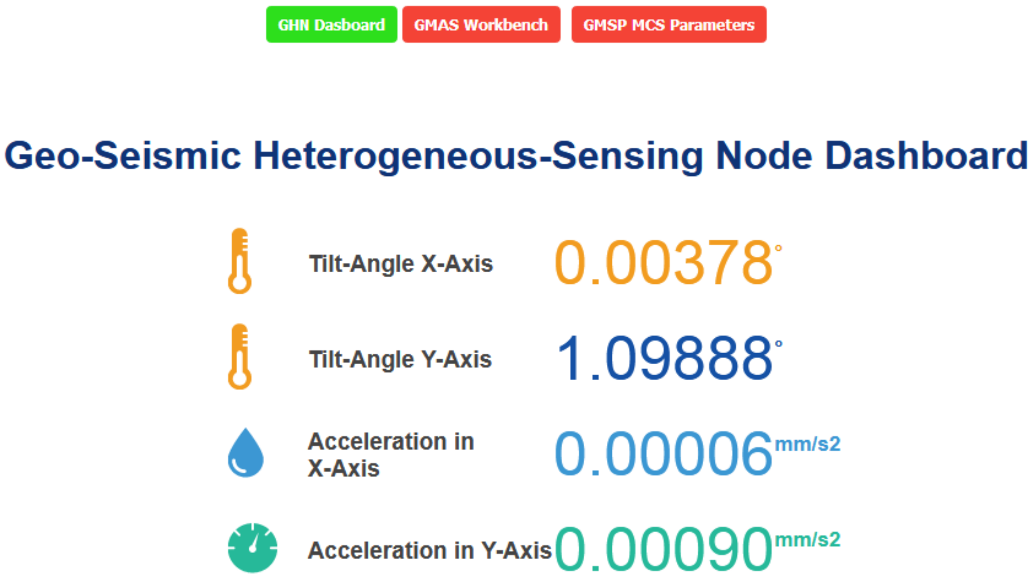

Figure 14. IoT Web GHN Dashboard

The first page is the GHN dashboard page as shown in figure 14 with a refresh rate of 100Hz. These values have to be almost zero to start the operation of GMSP. It needs a 10 to 20 min calibration in the worst case as SMA neutralizer self-calibrates the GMSP bed to achieve zero offset condition. The results were observed from two sources, i.e. the Tektronix oscilloscope and MATLAB serial input. The GMSP results are very fertile and perceivable by seismologists and geologists.

Preprints (www.preprints.org) | NOT PEER-REVIEWED | Posted: 29 July 2019 doi:10.20944/preprints201907.0324.v1

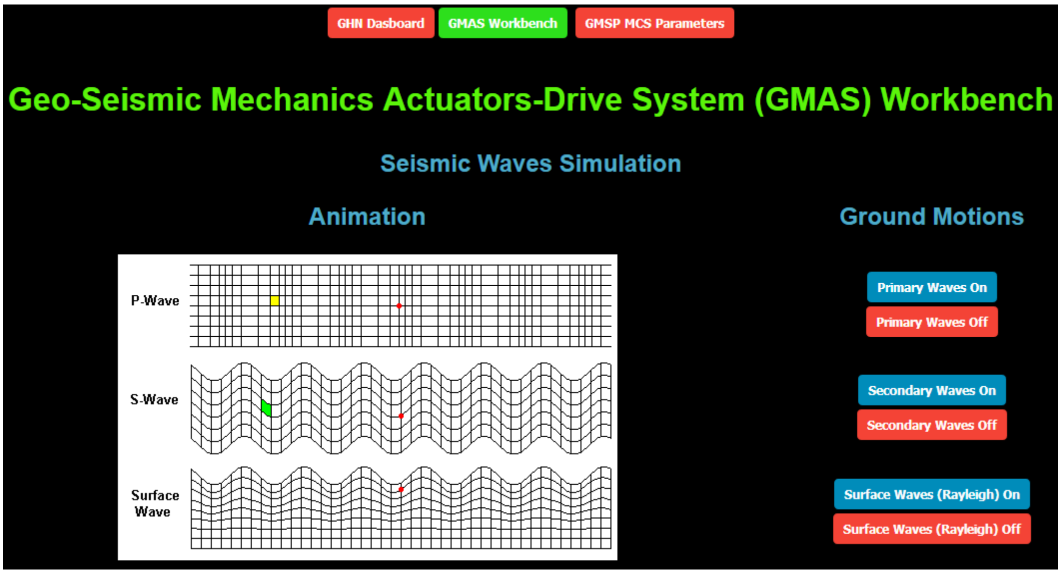

Figure 15. IoT Web GMAS Workbench – Seismic Wave Simulation (Top section)

This is a static page i.e. Page 2 shown in figure 15. Just press web buttons and start operations. The active operation button turned green. The P, S and surface waves are simulated just by pressing buttons according to the given parameters in Page 3.

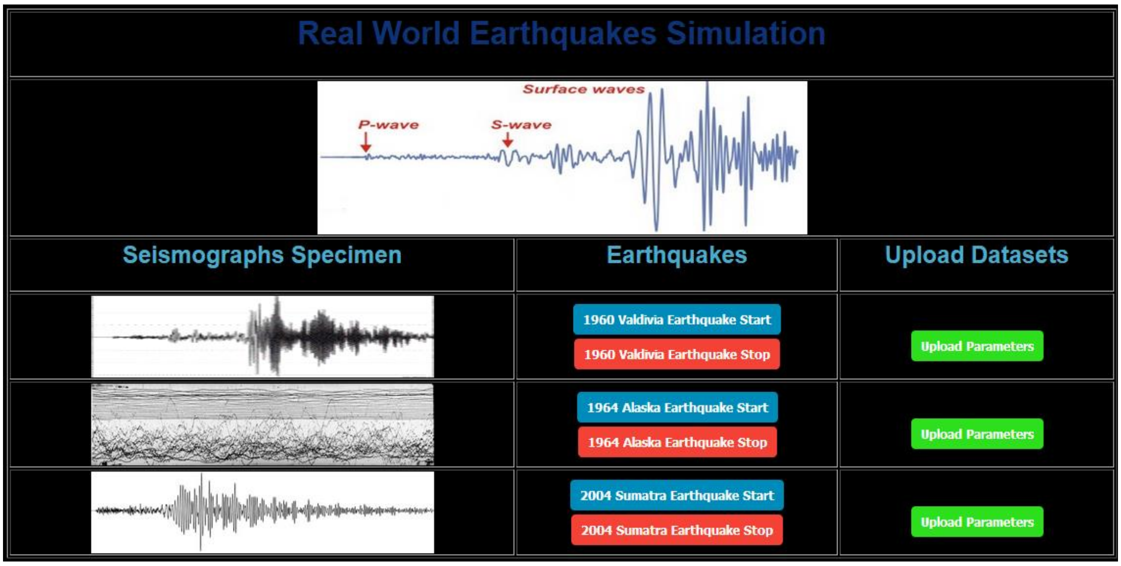

Figure 16. IoT Web GMAS Workbench – Earthquake Simulation (Bottom section)

The second section of Page 2 is shown in figure 16 i.e. dedicated for earthquake simulation. The green color of a button means "No Datasets Loaded". Upon loading the buttons became blue. One of the key work in GMSP is designed a native IRIS and USGS dataset converter on a chip that can load live data from the cloud and simulate it on the go.

Preprints (www.preprints.org) | NOT PEER-REVIEWED | Posted: 29 July 2019 doi:10.20944/preprints201907.0324.v1

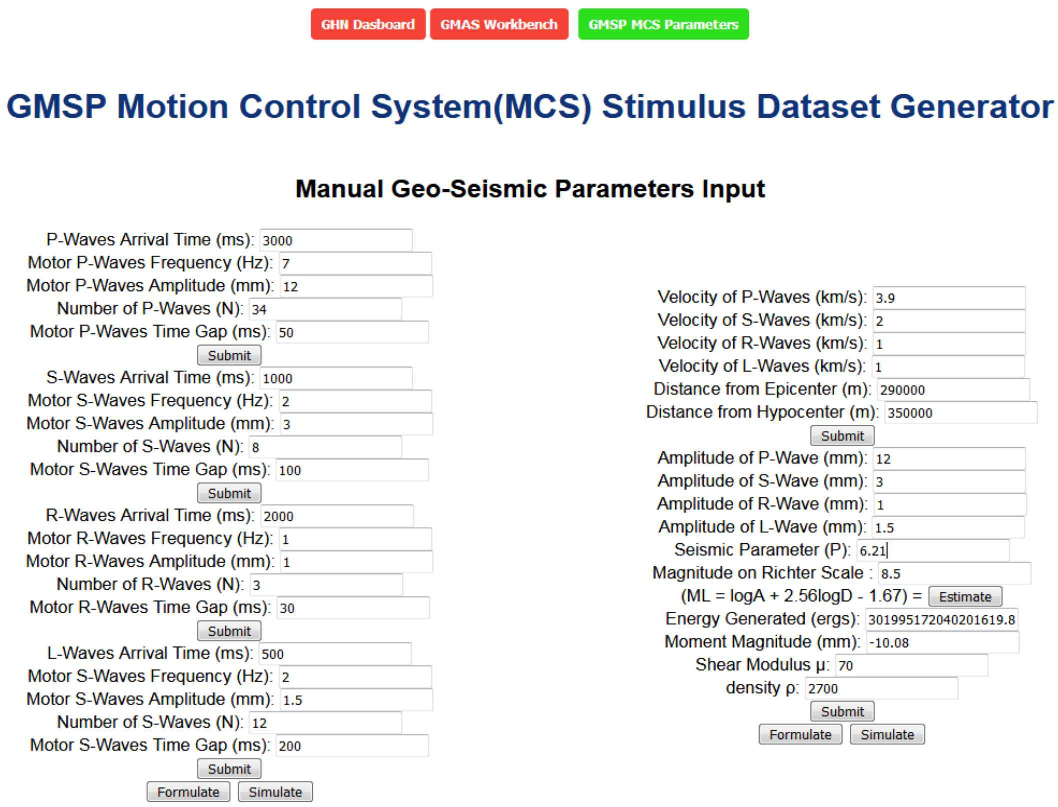

Figure 17. IoT Web GMAS Workbench – Seismic Wave Simulation (Top section)

The customized parameters input for GMSP to create seismic waves as well as the earthquake of any type that covers the safety and integrity of the motorized system as shown in figure 17. Page 3 creates a motor command file on SPIFFS that stays that there deleted. These values become the right hand side variables of GRE.

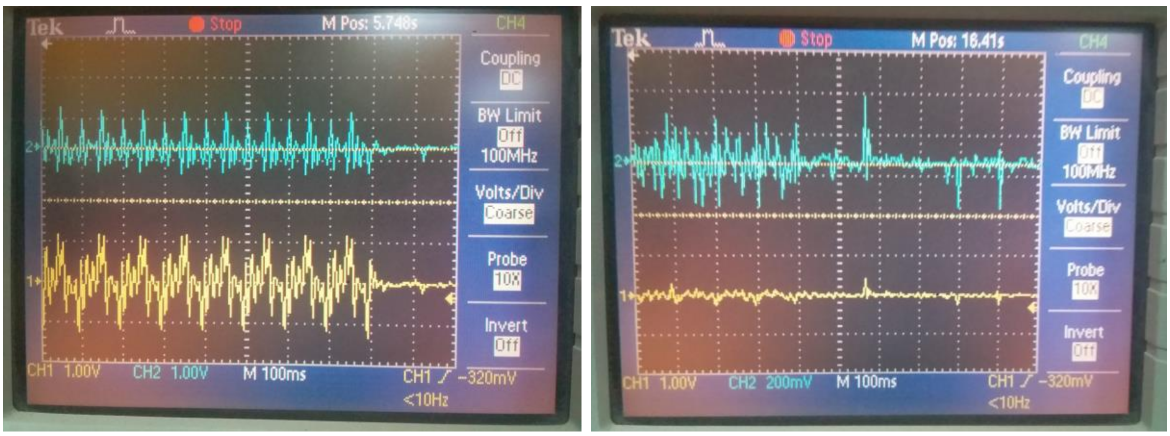

(**a**) (**b**)

Figure 18. Observations of GMSP Simulation from Tektronix 2014 Oscilloscope as (**a**) P-Wave with 10.3mm Wavelength at 8 Hz; and (**b**) S-Wave with 17mm wavelength at 4 Hz.

The results on the oscilloscope are very self-explanatory where the yellow line is for x-axis or vertical motion and cyan line for y-axis or horizontal motion. The frequencies achieved by the system are almost ideal and very accurate as shown in figure 18. The P-wave crust and trough is very extremely high and prominent with time period 100ms and unit segment of oscilloscope ±1.6V_{PK-PK} covers 80% of the x-axis as proof of 8Hz frequency in figure 18(a). The s-wave is being measured at the same settings except that the unit division is 200mV i.e. total of 5 divisions on the y-axis and slight variation of ±10mV on the x-axis in figure 18(b).

Preprints (www.preprints.org) | NOT PEER-REVIEWED | Posted: 29 July 2019 doi:10.20944/preprints201907.0324.v1

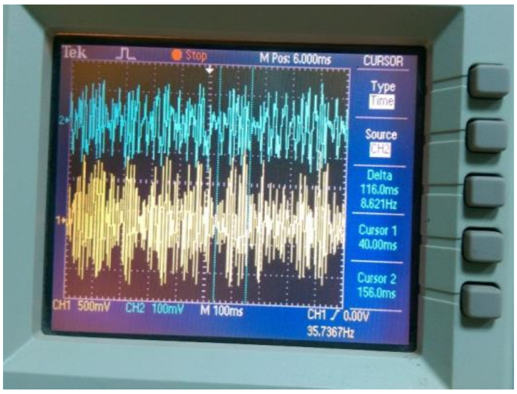
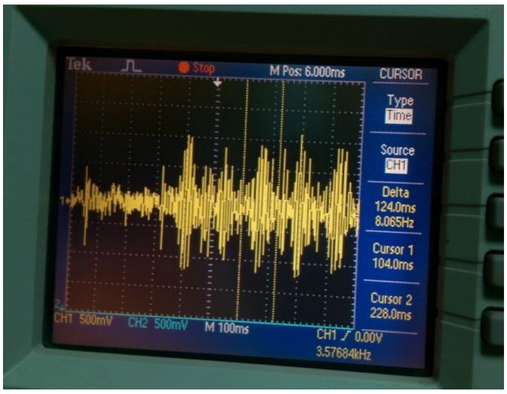

(**a**) (**b**)

Figure 19. Observations of GMSP Simulation observed from Tektronix 2014 Oscilloscope as (**a**) R-Wave with 16.03mm Wavelength at 35.73 Hz; and (**b**) L-Wave with 1.7mm wavelength at 78.092 Hz.

The results for R and L waves on the oscilloscope are very self-explanatory in figure 19. The frequencies achieved by the system i.e. 35Hz+ and 78Hz+ are extremely high and show the capability of the system to generate 10 times faster frequencies that were not observed in the literature before for R and L waves. The value 3.57684kHz is due to motor internal vibration when overstepped and accelerated to above final limits and creates plenty of pseudo-random noise that can be observed in the signal.

A much detailed observation of figure 19 (a) shows that R wave motion is translating along x-axis showing ±2.5 $V_{PK\text{-}PK}$ at 500mV grid setting i.e. slightly higher than the y-axis ±2.2 $V_{PK\text{-}PK}$ at 1V grid setting. In figure 19 (b) its only z-axis motion by changing the orientation of GHN on GMSP bed i.e. showing ±2.1 $V_{PK\text{-}PK}$ at 500mV grid setting. This surface motion is much challenging to produce as is only in one axis rest axis contain noise only.

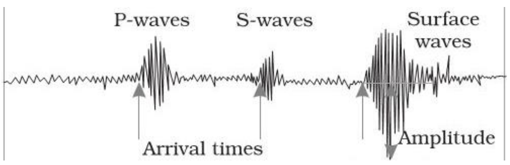

(**a**) (**b**)

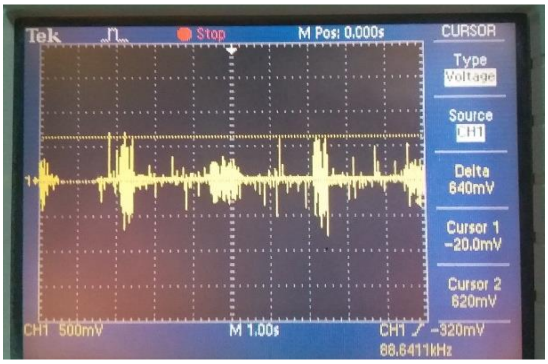
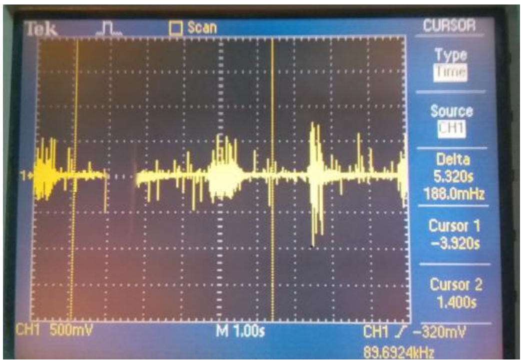

(**a**) (**d**)

Figure 20. Comparison of Characteristic Earthquake and Simulated Earthquake as (**a**) Standard Earthquake Pattern; (**b**) GMSP Simulated Pattern; (**c**) GMSP Generated Medium Earthquake Pattern; and (**d**) GMSP Generated High Earthquake Pattern.

doi:10.20944/preprints201907.0324.v1

The GMSP generated different earthquakes by varying the frequency as well as the amplitude of displacement as shown in figure 19. The characteristic earthquake pattern has used a masterpiece for simulation and all the patterns shown in figure 20 from (a) to (b) are by studying different datasets mentioned in the literature review. The duration of an earthquake is 8s in figure 20 (a) i.e. 1s to 9s on scope, P-waves arrival after 2s, S-waves after 4s and surface waves after 6s. Two earthquakes in figure (c) with duration 5.5 seconds without gap i.e. from 1.5s to 6s for first and 6s to 10s for the second earthquake with a 100mV amplitude of P-wave, 320mV for S-wave and 505mV for surface waves. The numbers 7.73085kHz, 88.6411kHz, and 89.6924kHz are due to pseudo-random noise produced by stepper motors being a different research domain in electro-mechanical engineering.

The serial out of the ESP32 was connected to PC for observations in MATLAB. The results in MATLAB were digital and had a lesser impact of pseudo-random noise observed in TDS 2014.

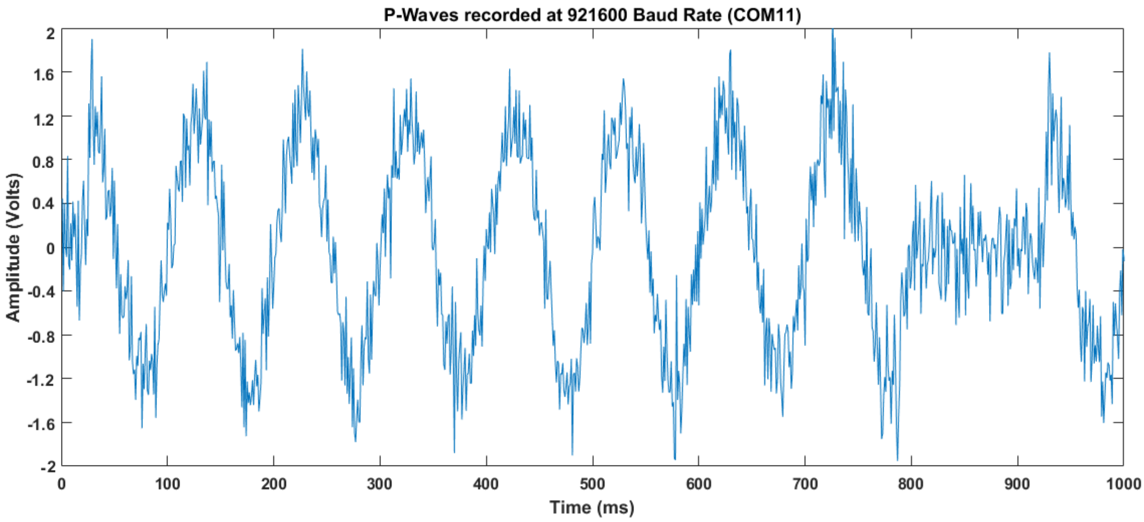

Figure 20. P-Waves observed in MATLAB for 8Hz on the x-axis

First, figure 18 (a) code was simulated and $\pm 1.6V_{PK-PK}$ curves were observed in MATLAB by only considering the x-axis acceleration signal. The plot captured data trace shows a significant difference in clarity in digital and analog data processing outputs.

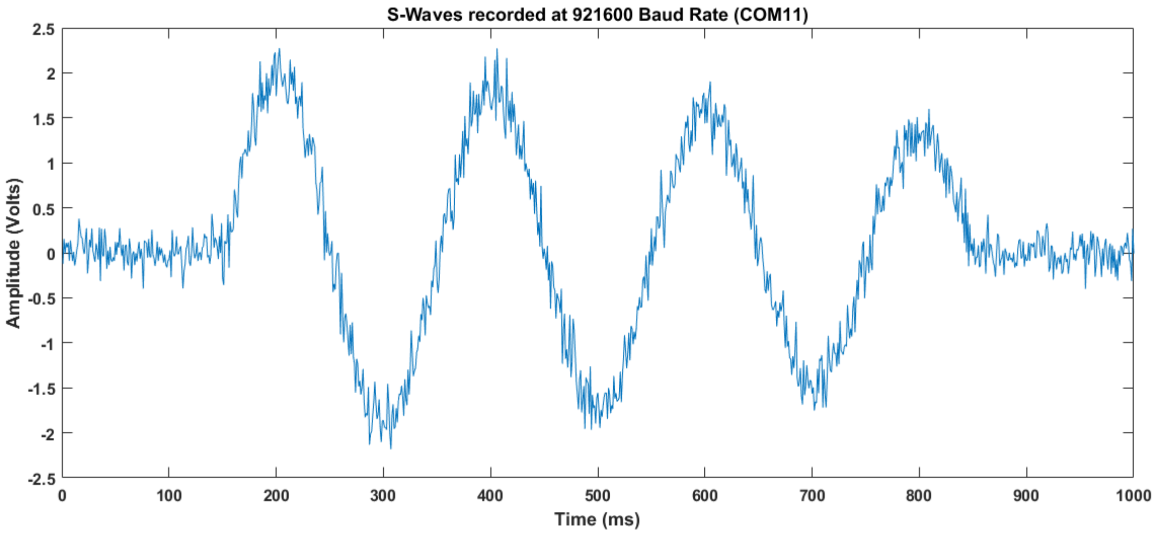

Figure 21. S-Waves observed in MATLAB

Furthermore, figure 18 (b) code was simulated and ±2.2VPK-PK curves were observed in MATLAB. The 200mV grid setting plot on the 2000ms scale on TDS 2014 displayed as figure 21 in MATLAB as a 1000ms scale for y-axis signal to demonstrate vertical ground motion capabilities.

 doi:10.20944/preprints201907.0324.v1

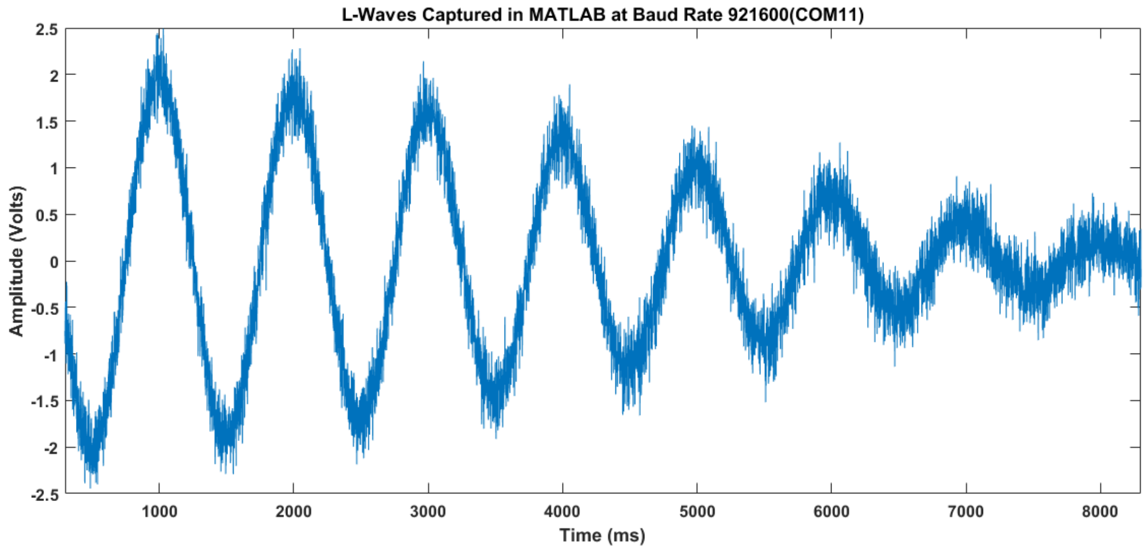

Figure 22. L-Waves observed in MATLAB at 1Hz

GMSP simulated L-wave with time period T_L>1.1s can be observed in MATLAB for custom parameters given in GMSP MCS stimulus page as shown in figure 22. The eight waves traveling over the crust can be observed in figure 22. The gradual degradation or depreciation in amplitude and time period of all the seismic waves is to seismic parameter Ψ dependent on the elasticity of and density of medium or stress and strain bearing capacity of the medium. In this simulation Ψ = 6.21 has been used.

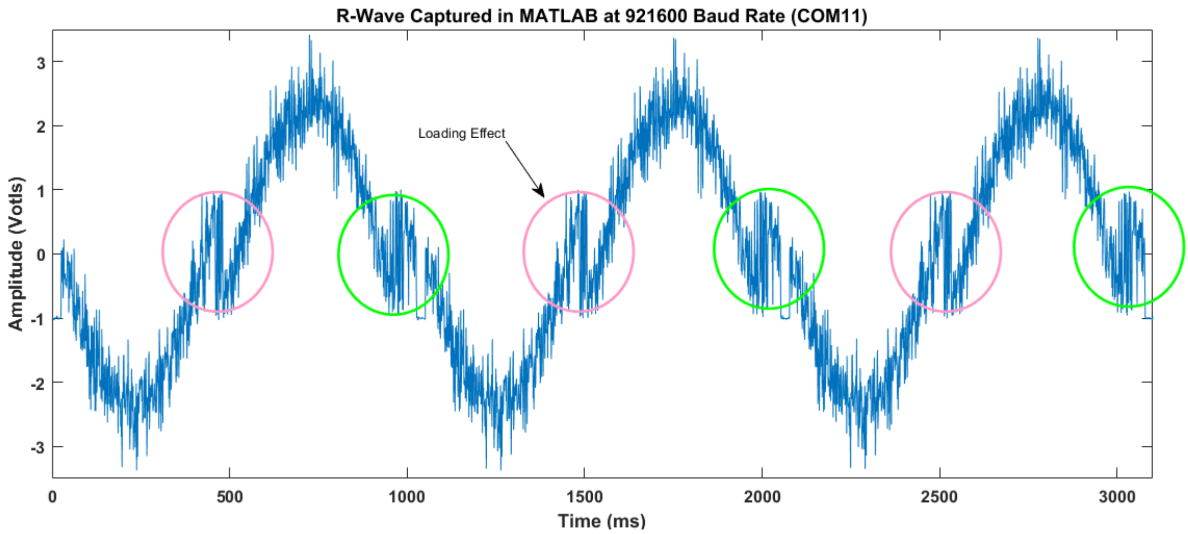

Figure 23. R-Waves observed in MATLAB

Figure 23 is based on R-wave simulation at Ψ = 6.21 and with the time period of T_R = 1s. The circles show the loading effect of motors and axis at a point where x-axis and y-axis motion merges or maximum x-axis value for a given y-axis i.e. when y-axis displacement just about to converge or touch the x-axis displacement its green and when y-axis about to diverge its purple means more y-axis and less x-axis means anti-clockwise in both scenarios.

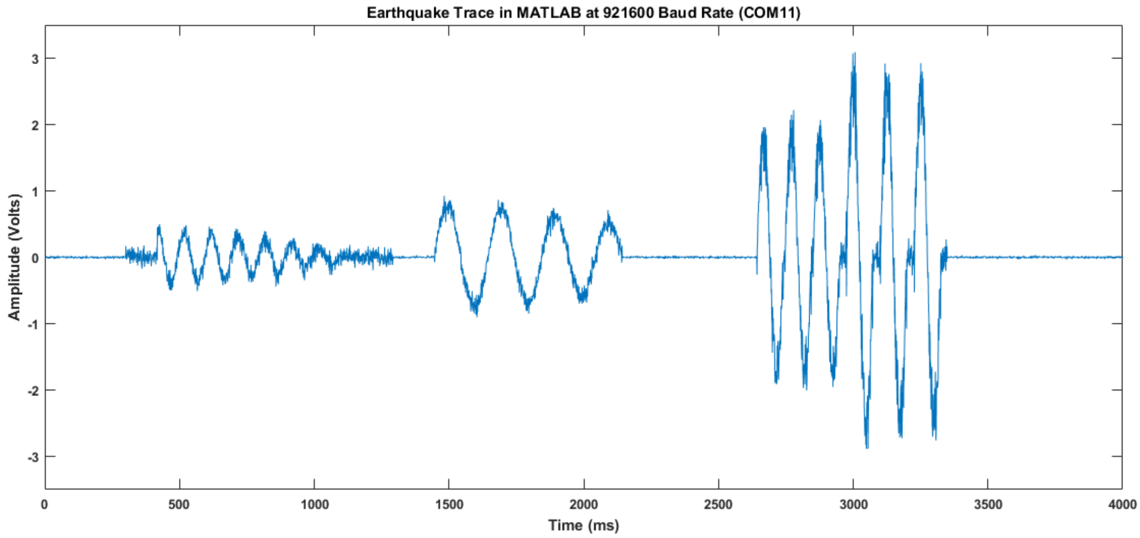

Figure 24. GMSP simulated Earthquake captured in MATLAB (4 seconds)

An earthquake comprised of eight P-waves of $\pm 0.4V_{PK-PK}$ amplitude and frequency 8Hz in the x-axis, four S-waves with $\pm 1V_{PK-PK}$ amplitude and frequency 4 Hz in the y-axis, three L-waves with $\pm 2.1V_{PK-PK}$ amplitude in the y-axis and three R-waves with $\pm 2.5V_{PK-PK}$ amplitude in z-axis were simulated based on standard earthquake seismograph.

6. Conclusions

A multi-parametric five degree-of-freedom seismic wave ground motions simulation platform for P, S, L and R seismic waves was designed, fabricated, assembled, programmed and tested for multiple ground motions i.e. at different frequencies, amplitudes, patterns, arrival times of seismic events. The possible minima and maxima were tested and results show that GMSP can serve as a reliable source for remote earthquake simulation and detection as global scale AI and machine learning platform. The results show the significance of GMSP for geo-physicists especially seismologists, a new era for motion control system developers, virtual reality and augmented reality scientists and data scientists to test their datasets. The platform was successful in emulating standard as well as extreme ranges of seismic frequencies, displacements, and velocities at given seismic parameters in addition to possible theoretical estimations in geo-seismic systems. Architects and construction engineers can use this platform to improve their realization for seismic-tolerant design and advise better structural optimization and material specifications to meet the acoustic analysis demands. This system can also record the ground motion and then simulate it again through SMA and GCS. This constitutes a strong tool to train algorithms for machine learning and AI as well as deep learning models. The limitation of this system in this version is stepper motor vibration noise observed in all plots, the IRIS, and USGS datasets need to be converted into GMSP motor command file before feeding to GRE and structural mounting assembly on surface waves sub-section to observe the behavior or micro-models of structures.

Author Contributions: Conceptualization, H.T.; Data curation, H.T.; Formal analysis, H.T.; Funding acquisition, F.T., M.A.E.A.-H., D.C. and A.B.M.; Investigation, H.T; Methodology, H.T.; Project administration, F.T.; Resources, F.T., M.A.E.A.-H., D.C. and A.B.M.; Software, H.T.; Supervision, F.T.; Validation, H.T.; Visualization, H.T.; Writing—original draft, H.T.; Writing—review & editing, F.T., M.A.E.A.-H., D.C. and A.B.M.

Funding: This publication was made possible by NPRP grant # 8-1781-2-725 from the Qatar National Research Fund (a member of Qatar Foundation). The publication of this article was funded by the Qatar National Library. The statements made herein are solely the responsibility of the authors.

Conflicts of Interest: The authors declare no conflict of interest. The funders had no role in the design of the study; in the collection, analyses, or interpretation of data; in the writing of the manuscript, or in the decision to publish the results.

Preprints (www.preprints.org) | NOT PEER-REVIEWED | Posted: 29 July 2019 doi:10.20944/preprints201907.0324.v1

References

1. Debarati, G.; Philippe, H.; Pascaline, W.; and Regina, B. Annual Disaster Statistical Review 2016: The numbers and trends, *Centre for Research on the Epidemiology of Disasters (CRED)*, 2016.
2. Suzette, K. Earthquake Statistics. *United States Geological Survey*, 2017.
3. Keith, R. D.; and James, H. D. RSQSim Earthquake Simulator. *Seismological Research Letters*, 2012.
4. Steven, N. W. ALLCAL Earthquake Simulator. *Seismological Research Letters*, 2012.
5. Fred F. P. A Viscoelastic Earthquake Simulator with Application to the San Francisco Bay Region. *Bulletin of the Seismological Society of America*, 2009.
6. Mark, R. Y; Kasey, W. S.; Eric, M. H.; John,B. R.; Donald, L. T.; Jay, W. P.; and Andrea, D. The Virtual Quake earthquake simulator: a simulation-based forecast of the El Mayor-Cucapah region and evidence of predictability in simulated earthquake sequences Earthquake Simulator. *Geophysical Journal International*, 2015.
7. Shunsuke, H.; Kohei, F.; Tsuyoshi, I.; Muneo, H.; Seckin, C.; and Takane, H. A physics-based Monte Carlo earthquake disaster simulation accounting for uncertainty in building structure parameters. *Fourteenth International Conference on Computational Science*, 2014.
8. Muneo, H.; and Tsuyoshi, I. Current state of integrated earthquake simulation for earthquake hazard and disaster. *Journal of Seismology*, 2007.
9. Terry, E. T.; Keith, R. D.; Michael, B; James, H. D.; Edward H. F.; Eric M. H.; Louise, H. K.; Fred F. P.; John B. R; Michael, K. S; Donald, L. T.; Steven, N. W.; and Burak, Y. Generic Earthquake Simulator. *Seismological Research Letters*, 2009.
10. Alkut, A. A new 3-D Earthquake Simulator for Training and Research Purposes. *Thirteenth World Conference on Earthquake Engineering*, 2010.
11. Keiichi, O.; Toru, H.; Nobuyuki, O.; and Masayoshi, S. Project on 3-D Full-Scale Earthquake Testing Facility. *Fourth Report*, 2006.
12. Kai-Chao, Y.; Wei-Tzer, H.; Cheng-Lung, L.; Pei-En, W. U.; and Jiunn-Shean, C. Virtual Instrumentation Design on Earthquake Simulation System. *International Conference on Artificial Intelligence and Industrial Engineering(AIIE)*, 2015.
13. Velikoseltsev, A.; Alexander, Y.; and Khvostov, V. Implementation of the high accuracy variable rotation testbench: seismology options. *Fourth IWGoRS*, 2016.
14. A.N Swaminathen, P.Sankari. Experimental Analysis of Earthquake Shake Table. *American Journal of Engineering Research(AJER)*, 2017.
15. Weixing, S. Shaking Table Experimental Study of Reinforced Concrete High-Rise Building. *Twelfth WCEE*, 2000.
16. Jordan, E. B. Seismic Modeling with an Earthquake Shake Table, *DigitalCommons*, 2012.
17. Shiling, P.; John, V. L.; Andre, R. B.; Jeffrey, B.; Hans, E. B.; James, D.; Eric, M.; Reid, Z.; Massimo, F.; and Douglas, R. Full-Scale Shake Table Testing of a Two Storey Mass-Timber Building with Resilient Rocking Wall Lateral System. *Sixteenth European Conference on Earthquake Thessaloniki Engineering*, 2017.
18. Renann, G. B.; and Elmer, P. D. Design and Development of a Fuzzy-PLC for an Earthquake Simulator / Shake Table. *Seventh International Conference Humanoid, Nanotechnology, Information Technology Communication and Control, Environment and Management (HNICEM)*, 2017.
19. Narutoshi, N. A multi-purpose earthquake simulator and a flexible development platform for actuator controller design. *Journal of Vibration and Control*, 2017.

 doi:10.20944/preprints201907.0324.v1

20. Farid, T.; Hasan, T.; Damiano, C.; and Adel, B. M. Design and Simulation of a Green Bi-Variable Mono-Parametric SHM Node and Early Seismic Warning Algorithm for Wave Identification and Scattering. *Fourteenth International Wireless Communications & Mobile Computing Conference(IWCMC)*, 2018.
21. Farid, T.; Hasan, T.; Mohammed, A. A.; Adel, B. M.; Anas, T.; and Damiano, C. IoT and IoE prototype for scalable infrastructures, architectures and platforms. *International Robotics & Automation Journal*, 2018.
22. Hasan, T.; Anas, T.; Farid. T.; Mohammed, A. A.; Adel, B. M.; and Damiano, C. Geographical Area Network—Structural Health Monitoring Utility Computing Model. *International Journal of Geo-Information*, 2018.
23. Hasan, T.; Anas, T.; Farid. T.; Mohammed, A. A.; Adel, B. M.; and Damiano, C. Structural Health Monitoring Installation and Deployment Scheme using Utility Computing Model. *Second European Conference(EECS)*, 2018.
24. Hasan, T.; Farid, T.; Damiano, C.; and Adel, B. M. Design and Implementation of Programmable Multi-Parametric 4-Degrees of Freedom Seismic Waves Ground Motion Simulation IoT Platform. *Fifteenth International Wireless Communications & Mobile Computing Conference(IWCMC)*, 2019.
25. Hasan, T.; Anas, T.; Farid. T.; Mohammed, A. A.; Adel, B. M.; and Damiano, C. Design and Implementation of Information Centered Protocol for Long Haul SHM Monitoring. *International conference on Design and Test of Integrated Micro and Nano-Systems(DTS)*, 2019.